JACS
JOURNAL OF THE AMERICAN CHEMICAL SOCIETY
Article
pubs.acs.org/JACS

# Insights into the Interplay of Lewis and Brønsted Acid Catalysts in Glucose and Fructose Conversion to 5-(Hydroxymethyl)furfural and Levulinic Acid in Aqueous Media

Vinit Choudhary,[†] Samir H. Mushrif,[‡] Christopher Ho,[†] Andrzej Anderko,[§] Vladimiros Nikolakis,[†] Nebojsa S. Marinkovic,[†] Anatoly I. Frenkel,[⊥] Stanley I. Sandler,*[,†] and Dionisios G. Vlachos*[,†]

[†]Center for Catalytic Science and Technology and Catalysis Center for Energy Innovation, Department of Chemical & Biomolecular Engineering, University of Delaware, Newark, Delaware 19716, United States

[‡]School of Chemical and Biomedical Engineering, Nanyang Technological University, 62 Nanyang Drive, Singapore 637459

[§]OLI Systems Inc., 108 The American Road, Morris Plains, New Jersey 07950, United States

[⊥]Physics Department, Yeshiva University, 245 Lexington Avenue, New York, New York 10016, United States

Supporting Information

**ABSTRACT:** 5-(Hydroxymethyl)furfural (HMF) and levulinic acid production from glucose in a cascade of reactions using a Lewis acid ($CrCl_3$) catalyst together with a Brønsted acid (HCl) catalyst in aqueous media is investigated. It is shown that $CrCl_3$ is an active Lewis acid catalyst in glucose isomerization to fructose, and the combined Lewis and Brønsted acid catalysts perform the isomerization and dehydration/rehydration reactions. A $CrCl_3$ speciation model in conjunction with kinetics results indicates that the hydrolyzed Cr(III) complex $[Cr(H_2O)_5OH]^{2+}$ is the most active Cr species in glucose isomerization and probably acts as a Lewis acid−Brønsted base bifunctional site. Extended X-ray absorption fine structure spectroscopy and Car−Parrinello molecular dynamics simulations indicate a strong interaction between the Cr cation and the glucose molecule whereby some water molecules are displaced from the first coordination sphere of Cr by the glucose to enable ring-opening and isomerization of glucose. Additionally, complex interactions between the two catalysts are revealed: Brønsted acidity retards aldose-to-ketose isomerization by decreasing the equilibrium concentration of $[Cr(H_2O)_5OH]^{2+}$. In contrast, Lewis acidity increases the overall rate of consumption of fructose and HMF compared to Brønsted acid catalysis by promoting side reactions. Even in the absence of HCl, hydrolysis of Cr(III) decreases the solution pH, and this intrinsic Brønsted acidity drives the dehydration and rehydration reactions. Yields of 46% levulinic acid in a single phase and 59% HMF in a biphasic system have been achieved at moderate temperatures by combining $CrCl_3$ and HCl.

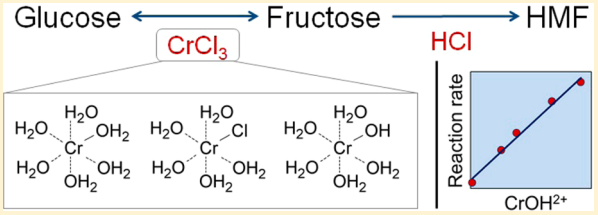


## INTRODUCTION

The diminishing availability of petroleum reserves and growing environmental concerns over greenhouse gas emissions have spurred research into utilizing biomass as a feedstock for the production of chemicals and transportation fuels.[1−5] A major challenge is developing economic, efficient, and environmentally benign technologies to transform lignocellulosic biomass into fuels and chemicals. Consequently, cellulosic biomass conversion to platform chemicals, such as 5-(hydroxymethyl)furfural (HMF) and levulinic acid, has recently gained significant attention.[6−12]

HMF is produced from the dehydration of hexose sugars, such as glucose and fructose, and is envisaged as a potential platform chemical for the biofuel, biochemical, and biopolymer industries.[3,8,9,13−22] HMF derivatives, such as 2,5-dimethylfuran and 5-(ethoxymethyl)furfural, have been reported as promising biofuel components.[23,24] 2,5-Furandicarboxylic acid, produced by the oxidation of HMF, can substitute for terephthalic acid in the production of polyesters such as polyethylene-furanoate and other polymers containing an aromatic moiety.[25] HMF hydrolysis produces levulinic acid, which can be used to produce a variety of products, e.g., acrylate polymers and fuel additives such as γ-valerolactone, 2-methyl-tetrahydrofuran, and ethyl levulinate.[12]

High yields of HMF from fructose have been reported in aqueous media,[14,26−28] organic solvents,[29−33] and ionic liquids.[22,34,35] However, fructose is not an ideal feedstock for HMF production due to its high cost.[36] The cost of glucose is about half that of fructose; as a result, glucose isomerization to fructose followed by its subsequent dehydration to HMF in a one-pot synthesis has recently gained attention. High yields of HMF from glucose have been reported in ionic liquids[22,37−39] and organic solvents,[40−43] particularly using various metal salts as catalysts for the glucose (aldose)-to-fructose (ketose) isomerization. However, the efficient downstream separation

**Received:** December 16, 2012
**Published:** February 22, 2013

   dx.doi.org/10.1021/ja3122763 | J. Am. Chem. Soc. 2013, 135, 3997−4006

of HMF from high-boiling organic solvents or ionic liquids, and the recycling of the reaction media, pose challenges to the commercialization of these processes. Consequently, water appears to be a better choice for HMF production. Recently, the Sn-$\beta$ zeolite has been demonstrated to be an efficient catalyst for the aldose-to-ketose isomerization reaction in aqueous media.[44−46] An HMF yield of ∼57% with a glucose conversion of ∼80% at 453 K using a combination of Sn-$\beta$ and HCl as catalysts has been reported.[47]

Typically, heterogeneous catalysis is preferred over homogeneous catalysis because of the ease of catalyst separation and its reusability. However, the formation of unwanted side products, such as soluble polymers and humins, which can deposit in the catalyst pores, requires frequent catalyst regeneration. This suggests a need to explore homogeneous catalytic processes for HMF production from glucose in aqueous media.

In the past, various metal salts have been tested, and some of them, e.g., salts of Cr(III), Al(III), Zn(II), and Sn(IV), have been found to be active in HMF synthesis from glucose in aqueous media.[48−53] Recently a HMF yield of ∼60% was reported at 443 K using $AlCl_3$ and HCl as catalysts in aqueous media.[54] However, obtaining a high HMF yield from glucose at low to moderate reaction temperatures in aqueous media remains a challenge. Moreover, there is a need to establish a fundamental understanding of the role of metal salts in these reactions.

In this work we investigate the Lewis acid ($CrCl_3$)-catalyzed glucose transformation in aqueous media combined with a Brønsted acid (HCl) to produce HMF and levulinic acid. The glucose consumption kinetics in both single-phase and biphasic systems are reported, and the effect of intrinsic and extrinsic Brønsted acidity on the product of isomerization is elucidated. The effect of $CrCl_3$ on Brønsted acid-catalyzed fructose dehydration and HMF hydrolysis is also investigated. The $CrCl_3$ speciation in water is explored, and the glucose-to-fructose (or aldose-to-ketose) isomerization is correlated with various Cr species for the first time. Further, we report the first results of an extended X-ray absorption fine structure (EXAFS) study and Car−Parrinello molecular dynamics (CPMD) simulations to investigate the interaction of the key chromium ion, indicated from the kinetics experiments and speciation model, with the glucose molecule.

## METHODS

**Experimental Details.** The reactions were conducted using 10 mL thick-walled glass vials (Sigma-Aldrich) heated in a temperature-controlled oil bath on a digital stirring hot plate (Fisher Scientific). Glucose, fructose, mannose, HMF, levulinic acid, formic acid, $CrCl_3{\cdot}6H_2O$, and $CrCl_2$ were purchased from Sigma-Aldrich and were used as received. In a typical experiment, 2 mL of an aqueous solution of reactant (10 wt %) was added to the reactor that was then sealed. A Cr-to-reactant molar ratio of 3:100, which corresponds to a $CrCl_3$ concentration of ∼18.6 mM for 10 wt % glucose solution, was used in the kinetics measurements. The HCl concentration was fixed at 0.1 M when used with $CrCl_3$. Tetrahydrofuran (THF) was used as an extracting medium with an organic-to-aqueous volume ratio of 2:1 when biphasic systems were studied. An extra vial filled with heating oil was placed along with the reaction vials to record temperature during the reaction. Magnetic stirrers were used for mixing during reactions. The kinetics experiments were carried out using multiple vial reactors, which were taken out from the oil bath at specified times and immediately quenched to room temperature in water.

The liquid samples were analyzed with high-performance liquid chromatography (HPLC) using a Waters Alliance System instrument (e2695). The chromatograph is equipped with a refractive index detector and a photodiode array detector. Sugars were separated using two Biorad HPX87C (300 × 7.8) columns in series at a column temperature of 348 K with HPLC-grade water as mobile phase at a flow rate of 0.50 mL/min. Glucose, mannose, and fructose eluted at 23.3, 27.2, and 31.1 min, respectively. HMF, levulinic acid, and formic acid were separated from the reaction mixture using a Biorad HPX87H (300 × 7.8) column, with water (0.005 M sulfuric acid) as the mobile phase at a flow rate of 0.65 mL/min and a column temperature of 338 K. Formic acid, levulinic acid, and HMF eluted at 13.1, 14.7, and 28.1 min, respectively. During the HPLC analysis, the typical relative standard error was ∼1% for multiple injections from the same sample and ∼5−8% for replicate samples. Conversion of the reactant, yield, and selectivity of the products were calculated as follows:

$$\%\ \text{conversion of reactant} = \frac{(C_{\text{reactant},t=0} - C_{\text{reactant}})}{C_{\text{reactant},t=0}} \times 100$$

$$\%\ \text{yield of product } i = \frac{C_i}{C_{\text{reactant},t=0}} \times 100$$

$$\%\ \text{selectivity of product } i = \frac{C_i}{(C_{\text{reactant},t=0} - C_{\text{reactant}})} \times 100$$

Here, $C_i$ is the molar concentration of species $i$.

The Cr K-edge EXAFS analyses of aqueous $CrCl_3$ solutions with and without glucose were carried out at beamline X19A of National Synchrotron Light Source, Brookhaven National Laboratory. Samples were kept in a Kapton foil pouch, and the fluorescence signal was detected by a passivated implanted planar silicon detector (Canberra, USA). The monochromator was calibrated with a Cr foil, and the EXAFS data were analyzed using the IFEFFIT software package.[55,56] Theoretical EXAFS data for analyzing the nearest coordination environment around the central Cr atom in $CrCl_3$ solutions were constructed using FEFF6 code.[57] The atomic coordinates used in theoretical modeling were based on the structure of solid $Cr_2O_3$. It is assumed that the $CrCl_3{\cdot}6H_2O$ salt, since it is crystallized from a solution in which there are strong solute−solvent interactions, has Cr−O nearest-neighbor bonds in the local envinroment around Cr, thus resembling that in Cr oxide. Hence, the $Cr_2O_3$ compound can be used as the model structure for the local environment of the Cr(III) cations in solution. In the $Cr_2O_3$ structure, chromium is coordinated to six oxygen atoms in the first shell, in which three oxygen atoms in the first subshell are slightly closer than the three oxygen atoms from the second subshell (1.965 vs 2.016 Å). From the fit to the experimental data of bulk $Cr_2O_3$ oxide powders, the parameter $S_o^2$ was obtained, and its value (0.71) was used in further fittings of the solution data. It was also assumed that each Cr(III) ion remains coordinated to six water molecules with their oxygen end oriented toward the cation. Finally, to reduce the number of adjustable parameters, it was further assumed that the spread of Cr−O distances was small, and only one type of Cr−O bond, weighted by a coordination number, was used for the fit.

Dynamic light scattering (DLS) experiments on freshly prepared and heat-treated $CrCl_3$ solutions were carried out using a Brookhaven Instruments ZETAPALS instrument. The freshly prepared $CrCl_3$ solution was filtered using a syringe filter (200 $\mu$m), and then a portion of it was heated at 413 K for 3 h. DLS measurements were carried out both before heating and after heating of these samples without any further treatment. The autocorrelation functions were analyzed using the Multimodal Size Distribution algorithm of the accompanying software, assuming that the viscosity of the solutions was equal to that of water.

**Speciation Model.** $CrCl_3$ speciation in aqueous media was generated using the mixed-solvent electrolyte model of Wang et al.,[58−61] as implemented in the OLI Systems' Stream Analyzer software (OLI Systems, 2012). The details of these calculations are summarized in the Supporting Information.

**Car−Parrinello Molecular Dynamics Simulations.** The first-principles CPMD calculations were performed using the planewave−pseudopotential implementation of the density functional theory.[62] The simulation system consisting of $Cr(OH)^{2+}$, glucose molecule,

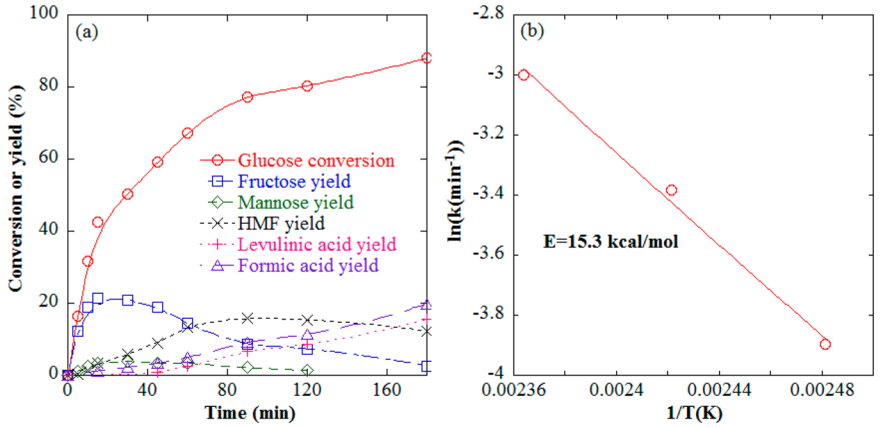


**Figure 1.** (a) Glucose conversion using $CrCl_3$ as a catalyst in an aqueous medium. (b) Arrhenius plot based on initial rate of glucose conversion. The estimated apparent activation energy ($E$) is 15.3 kcal/mol. Reaction conditions: initial reactant ~10 wt %, Cr to glucose molar ratio of 3:100, 413 K.

chloride ions, and water molecules was equilibrated for 0.5 ps at 350 K. Further technical details of CPMD simulations are included in the Supporting Information.

## RESULTS AND DISCUSSION

**Glucose Conversion Using a Lewis Acid Catalyst.** Figure 1a shows the time evolution of glucose consumption using a Lewis acid ($CrCl_3$) as a catalyst in aqueous media. $CrCl_3$ catalyzes glucose isomerization and forms fructose as the primary product together with a small amount of mannose. With time, the fructose concentration passes through a maximum, and HMF, levulinic acid, and formic acid are observed. HMF is produced by fructose dehydration and subsequently hydrolyzes to form levulinic and formic acids, as shown in Scheme 1. Both of these reactions are typically

**Scheme 1. Glucose Isomerization to Fructose and Its Transformation to HMF and Levulinic Acid**

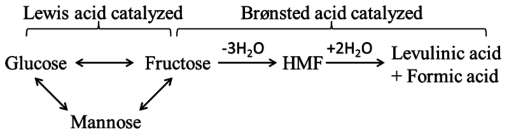


catalyzed by Brønsted acids. In order to understand why these products form, the pH of the solution was measured. The pH of the reaction solution was ~2.9 at the beginning of the reaction and ~1.6 at the end (measured by quenching the reaction sample to room temperature). It is clear that typical metal salts used for isomerization as Lewis acids render the solution fairly acidic. As a result, we hypothesize that the actual chemistry in these systems happens in a combined Lewis and Brønsted environment; the implications of this are discussed below. The source of this (intrinsic) Brønsted acidity when using $CrCl_3$ as a catalyst in water is investigated by modeling the $CrCl_3$ speciation in water, as discussed below in detail.

As typical in these reactions, significant carbon loss to unknown products was noticed. Most of the carbon loss during HMF and levulinic acid synthesis from hexoses is attributed to the formation of soluble polymers and insoluble humins, dark-colored tarry solids. Understanding and controlling these side reactions is a big challenge. Recently, some efforts have been made to analyze humins using infrared spectroscopy. It was suggested that aldol addition or condensation of 2,5-dioxo-6-hydroxyhexanal, an intermediate produced from HMF, is primarily responsible for the growth of humins.[63,64]

An apparent activation energy barrier of 15.3 kcal/mol is estimated for glucose isomerization from the initial kinetics, as shown in Figure 1b. This value agrees with our recently reported activation barrier (15.5 kcal/mol) for the isomerization of xylose, a pentose, using $CrCl_3$ as a catalyst in aqueous media;[65] it can be inferred that the activation barrier for $CrCl_3$-catalyzed aldose-to-ketose isomerization is nearly unaffected by the size of the sugar.

**Effect of Lewis Acidity on Fructose Dehydration and HMF Rehydration.** The chromium chlorides appear to be efficient catalysts for glucose isomerization; however, they alone do not appear to be very selective in the subsequent formation of HMF and levulinic acid. Therefore, a systematic study was conducted to understand the effect of $CrCl_3$ on the Brønsted acid-catalyzed fructose dehydration to HMF and HMF rehydration to levulinic acid.

The results from starting with fructose as a reactant using $CrCl_3$ as a catalyst are shown in Figure 2a. The initial fructose disappearance rate (0.043 $min^{-1}$) is faster than that of glucose (0.036 $min^{-1}$), as shown in Table 1. It should be noted that fructose not only isomerizes to glucose and mannose but also dehydrates to HMF in a parallel path. Moreover, $CrCl_3$ also catalyzes undesired side reactions involving fructose; this is further discussed below. The maximum HMF yield is higher (~21%) when starting with fructose than with glucose (~16%). Note that the glucose and mannose formation rates are very similar to each other when starting with fructose. This can be explained with our earlier proposed mechanism for aldose-to-ketose isomerization that suggests that the formation of glucose and mannose from fructose follows similar reaction pathways, and the only difference is which hydrogen atom on the C1-carbon of fructose is transferred to the C2 position in the isomerization pathway.[46]

Fructose dehydration was also carried out using HCl only, and HCl with $CrCl_3$, and the results from the two kinetics experiments are shown in Figure 2b and c, respectively. In these experiments, the pH was about 1. The presence of $CrCl_3$ does not alter the pH of the solution at these low values. It is evident (see Table 1) that the initial rate of fructose disappearance is faster in the presence of $CrCl_3$ with HCl (0.073 $min^{-1}$) compared to the only HCl case (0.035 $min^{-1}$). However, the maximum yield to HMF and levulinic acid drops from 39% to 28% and 60% to 47%, respectively. This indicates that $CrCl_3$


dx.doi.org/10.1021/ja3122763 | J. Am. Chem. Soc. 2013, 135, 3997−4006

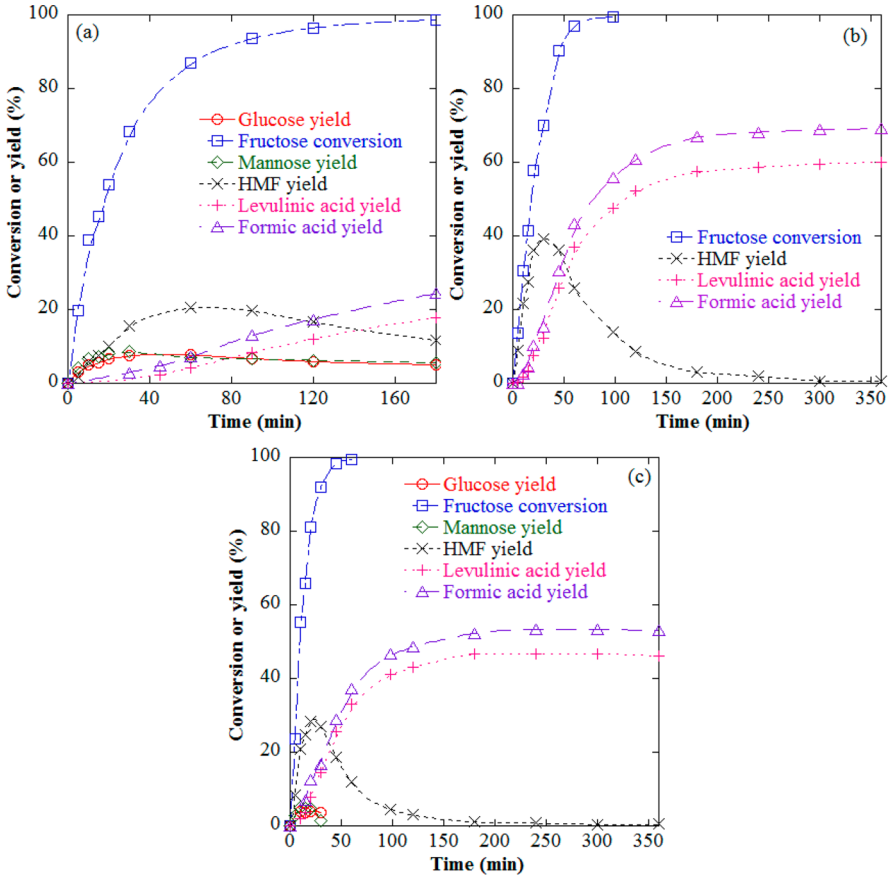


**Figure 2.** Fructose transformation to HMF and levulinic acid using (a) $CrCl_3$, (b) HCl, and (c) $CrCl_3$ with HCl as catalysts. Reaction conditions: initial reactant ~10 wt %, HCl (0.1 M, when used), Cr (when used)-to-fructose molar ratio of 3:100, and 413 K.

**Table 1. Reaction Rate Constants Associated with the Disappearance of Reactants in Various Reactions Carried Out at 413 K[a]**

| reactant | catalyst | $k$ ($min^{-1}$) | corresponding concentration profile |
|---|---|---|---|
| glucose | $CrCl_3$ | 0.036 | Figure 1a |
| glucose | $CrCl_3$, HCl | 0.024 | Figure 4a |
| glucose | $AlCl_3$ | 0.014 | Figure S1b |
| glucose | $AlCl_3$, HCl | 0.007 | Figure S1b |
| fructose | $CrCl_3$ | 0.043 | Figure 2a |
| fructose | HCl | 0.035 | Figure 2b |
| fructose | $CrCl_3$, HCl | 0.073 | Figure 2c |
| HMF | HCl | 0.012 | Figure 3a |
| HMF | $CrCl_3$, HCl | 0.016 | Figure 3b |

[a]The rate constants were obtained by fitting the initial concentration profiles (up to 15 min) of the reactant to a first-order reaction rate expression.

also catalyzes side reactions involving fructose, and hence adversely affects the yields of the desired products. In the case of only $CrCl_3$ (Figure 2a), the rate of fructose disappearance (0.043 $min^{-1}$) is faster than the only HCl case (Figure 2b) but slower compared to the combined $CrCl_3$ and HCl case (Figure 2c).

In order to understand the effect of $CrCl_3$ on HMF hydrolysis to levulinic and formic acids, a similar set of experiments was conducted starting with HMF, as shown in Figure 3. The addition of $CrCl_3$ accelerates the rate of HMF consumption compared to the HCl only case (see Table 1), and the maximum levulinic acid yield decreases from 82% in the only HCl case (Figure 3a) to ~72% in the case of HCl with $CrCl_3$ (Figure 3b).

Our data underscore that the intrinsic Brønsted acidity generated by $CrCl_3$ drives sufficient dehydration and rehydration reactions without external addition of Brønsted acid, and this needs to be accounted for in understanding the chemistry of sugars in water. This is consistent with the remarks made above in glucose chemistry. The above experiments indicate that the addition of $CrCl_3$ adversely affects both fructose conversion to HMF and HMF rehydration to levulinic and formic acids. These observations partly agree with an earlier reported observation that Lewis acidity in zeolites adversely affects xylose dehydration to furfural.[66] However, it should be noticed that not all Lewis acid sites are active for the aldose-to-ketose isomerization, and in that case, the Lewis acidity primarily catalyzes the undesired side reactions and adversely affects the formation of furfural and HMF from xylose and glucose, respectively.

In contrast, in our measurements, $CrCl_3$ is very active for aldose-to-ketose isomerization, as discussed above. Thus, using $CrCl_3$ in the aldose (glucose or xylose) conversion to its respective furan exhibits a trade-off between accelerating the rate of aldose-to-ketose isomerization and increasing the rate of formation of the undesired products. It should also be noticed that the selectivity to HMF increases in fructose dehydration with increasing temperature, indicating that the apparent activation energy associated with the HMF formation from fructose is higher compared with the side reactions.[19,27,67] An earlier study reported apparent activation barriers of 38.4, 27.5,


dx.doi.org/10.1021/ja3122763 | J. Am. Chem. Soc. 2013, 135, 3997−4006

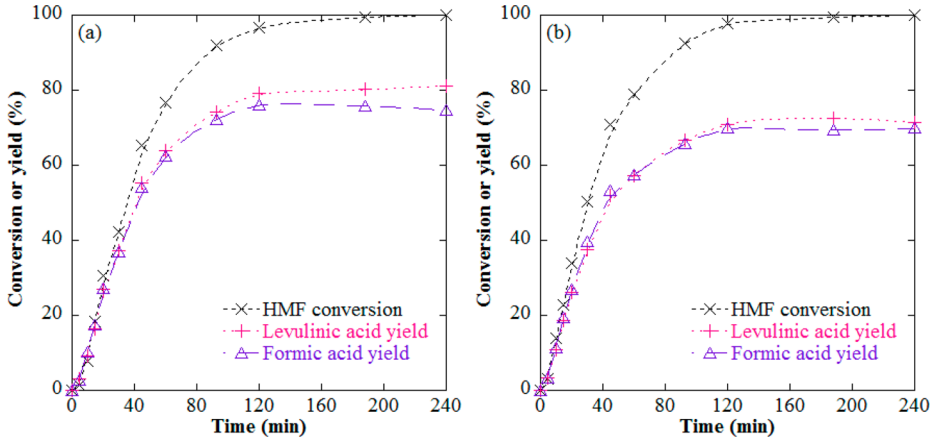


**Figure 3.** HMF transformation to levulinic and formic acids using (a) HCl and (b) HCl with $CrCl_3$ (Cr-to-HMF molar ratio of 3:100). Reaction conditions: initial reactant ~1 wt %, HCl (0.1 M), and 413 K.

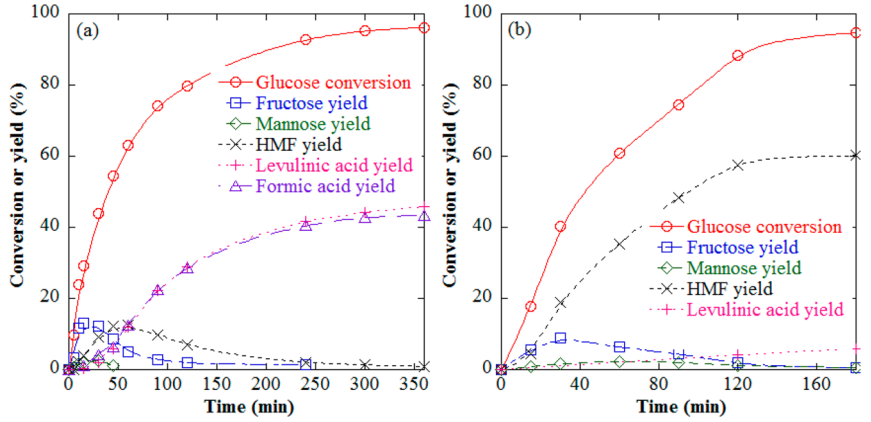


**Figure 4.** Glucose conversion and yield to various products using $CrCl_3$ and HCl in a single aqueous phase (a) and in a biphasic system (b). Reaction conditions: initial reactant ~10 wt %, HCl (0.1 M), Cr-to-glucose molar ratio of 3:100, and 413 K. In the biphasic system, THF was used as the organic solvent with the organic-to-aqueous phase volume ratio of 2:1, and 20 wt % NaCl in the aqueous media.

and 22.9 kcal/mol for HMF formation from fructose, levulinic acid formation from HMF, and HMF decomposition to the unknown side products, respectively.[68] Thus, it appears that HMF selectivity can be improved by either lowering the solution pH (increasing Brønsted acidity) or increasing the reaction temperature. We provide data in the next section that support this hypothesis.

**Effect of Extrinsic Brønsted Acid on Lewis Acid-Catalyzed Conversion of Glucose to HMF.** Next, we used HCl together with $CrCl_3$ in the glucose transformation to accelerate the fructose dehydration to HMF. Figure 4a shows the time evolution of the reactant and products in a single-phase aqueous medium. A yield of ~46% to levulinic acid is achieved in 360 min at 413 K in a single-phase aqueous system. This is the highest reported yield so far of levulinic acid from glucose at moderate reaction temperature in aqueous media. This shows that the use of a Lewis acid (in this case $CrCl_3$, which is active for aldose-to-ketose isomerization) in combination with a Brønsted acid can significantly improve yields of dehydration or rehydration products at the expense of side reactions driven by $CrCl_3$.

To further maximize the yield of HMF from glucose, we used an extractive-reaction process, where an organic solvent is used to extract HMF continuously from the aqueous media in a biphasic system.[8,14] It has also been reported earlier that addition of NaCl in the aqueous phase improves HMF partitioning between the organic and aqueous phases.[69] The glucose transformation using HCl and $CrCl_3$ as catalysts in the biphasic system with THF as the extracting medium and 20 wt % of NaCl in the aqueous phase is shown in Figure 4b. The glucose consumption rate in the biphasic system is similar to that in the single-phase reaction (e.g., ~41% glucose conversion (biphasic) compared to ~44% (single phase) in 30 min). The HMF partition coefficients (the ratio of the HMF concentrations in the organic media to the aqueous media) for various reaction samples were estimated to be about 7 from samples taken from the organic and aqueous phases. Overall, a high HMF yield of ~59% along with a ~7% yield of levulinic acid from glucose have been achieved in 180 min at a moderate reaction temperature of ~413 K in this biphasic system. When using a biphasic system, the aqueous phase can be recycled, so that the catalyst can be reused.

**$CrCl_3$ Speciation in Aqueous Media: Insights into the Combined Lewis and Brønsted Acid-Catalyzed Reactions.** To gain further insight into $CrCl_3$-catalyzed glucose-to-fructose isomerization and, more generally, into aldose-to-ketose isomerization (e.g., xylose to xylulose), we next considered the $CrCl_3$ speciation in water. In aqueous media, $CrCl_3$ dissociates to form ions. These ions are solvated by water and form complex ions, such as $[Cr(H_2O)_6]^{3+}$ (see next section about the first coordination sphere of the Cr ion as determined from EXAFS experiments). These ions can be further


dx.doi.org/10.1021/ja3122763 | J. Am. Chem. Soc. 2013, 135, 3997−4006

hydrolyzed, releasing $H^+$, resulting in a drop in the solution pH (for simplicity only a key reaction is shown here).[70]

$$[Cr(H_2O)_6]^{3+} + H_2O \leftrightarrow [Cr(H_2O)_5OH]^{2+} + H_3O^+ \quad (1)$$

The generated protons catalyze the fructose dehydration to HMF, and its subsequent hydrolysis to levulinic and formic acids, even when only $CrCl_3$ is used as a catalyst. Equation 1 provides, for the first time, the rationalization as to how Lewis acid catalysts (various salts) used for isomerization of aldoses to ketoses[48,54,65] drive Brønsted acid-catalyzed dehydration of ketoses to their corresponding furans. Since $CrCl_3$ dissolution results in the formation of various complex ions, understanding the speciation of $CrCl_3$ in aqueous media is required. Figure 5

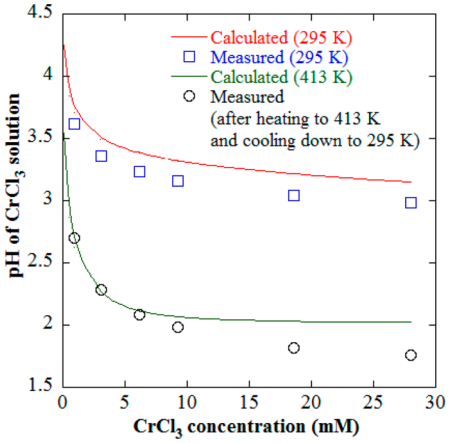


**Figure 5.** Comparison of the measured pH of aqueous solutions (symbols) of varying $CrCl_3$ concentrations with the pH values calculated using OLI software at 295 and 413 K.

compares the calculated pH with the measured pH as a function of $CrCl_3$ concentration at room temperature (295 K). The pH was measured after stirring the solution for 3 h at room temperature. The calculations are in good agreement with the measurements; the deviations in the pH values are slightly higher at high $CrCl_3$ concentrations. A notable observation is that, when the $CrCl_3$ solution is heated at 413 K for 1 h and then cooled to room temperature, the solution pH drops significantly and then remains unchanged, even after 192 h. Moreover, these pH values compare very well with the calculated values at 413 K, particularly at lower $CrCl_3$ concentrations, as shown in Figure 5. These observations suggest that the decrease in pH of the $CrCl_3$ solution at higher temperatures is largely an irreversible effect and can be attributed to the precipitation of $Cr(OH)_3$ as predicted by the $CrCl_3$ speciation calculations (see Supporting Information). We were not able to observe any $Cr(OH)_3$ particles with the naked eye. However, DLS measurements of heat-treated $CrCl_3$ solution revealed the presence of suspended particles. Since it was not possible to identify such particles in a freshly prepared sample, we can infer that the particle population observed in the heat-treated sample could be the $Cr(OH)_3$ predicted by the model. Importantly, our experiments and calculations predict that, as the $CrCl_3$ concentration increases, the intrinsic Brønsted acidity increases (eq 1), contributing to dehydration (of fructose) and rehydration (of HMF) reactions.

The $CrCl_3$ speciation was predicted at varying $CrCl_3$ concentrations (0.01−30 mM) at 295 and 413 K. The concentrations of various species, such as oxides, hydroxides, and chlorides of the chromium ion, are estimated; the thermodynamic distribution of these species strongly depends on the initial $CrCl_3$ concentration and the system temperature. The complete speciation results are tabulated in the Supporting Information. It is found that $[Cr(H_2O)_6]^{3+}$, $[Cr(H_2O)_5Cl]^{2+}$, and $[Cr(H_2O)_5OH]^{2+}$ account for most of the Cr (>99%) as shown in Figure 6, where these ions are represented as $Cr^{3+}$,

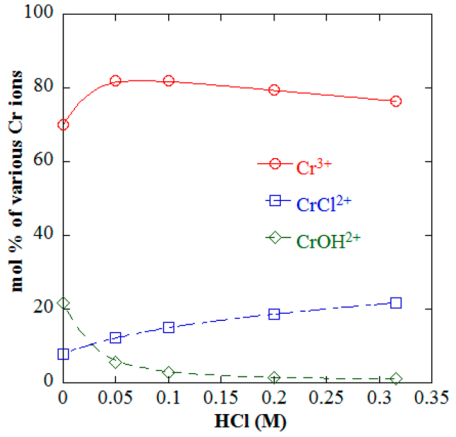


**Figure 6.** Effect of HCl addition on the species distribution in the $CrCl_3$ speciation (calculated using the OLI software) in aqueous media at 413 K.

$CrCl^{2+}$, and $CrOH^{2+}$, respectively. It is predicted that the concentration of $CrCl^{2+}$ and $CrOH^{2+}$ will increase with an increase in the solution temperature, except at very low $CrCl_3$ concentration (<3 mM), and is compensated by a decrease in the $Cr^{3+}$ concentration. The dominant complex ions of chromium in solution are shown in Scheme 2. It should be

**Scheme 2. Schematic Representation of the Key Cr(III) Cations Generated from the Dissolution of $CrCl_3$ in Aqueous Media**

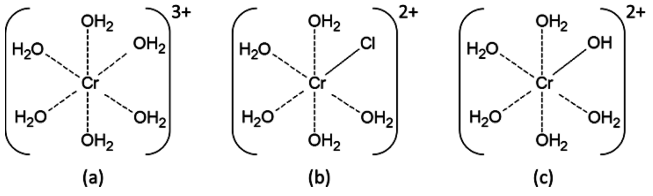


noticed that the chromium is present in the 3+ oxidation state in the aqueous solutions, which is a nontoxic state, and is in fact considered as an essential nutrient.[71]

The effect of HCl addition on the $CrCl_3$ speciation is shown in Figure 6. With increasing HCl concentration, the $CrCl^{2+}$ concentration increases monotonically, and that of $CrOH^{2+}$ decreases monotonically, whereas that of $Cr^{3+}$ first rises and then drops. The change in $CrCl_3$ speciation can be explained on the basis of the shifts in the thermodynamic equilibrium among various Cr species with increasing the concentration of $H^+$ and $Cl^-$, associated with an increase in HCl concentration. For example, an increase in $H^+$ concentration would shift the thermodynamic equilibrium toward the left (Le Chatelier's principle) in eq 1, and suppress the formation of $CrOH^{2+}$. In the kinetic experiments, the rate of glucose consumption drops significantly in the presence of $CrCl_3$ with the addition of HCl


dx.doi.org/10.1021/ja3122763 | J. Am. Chem. Soc. 2013, 135, 3997−4006

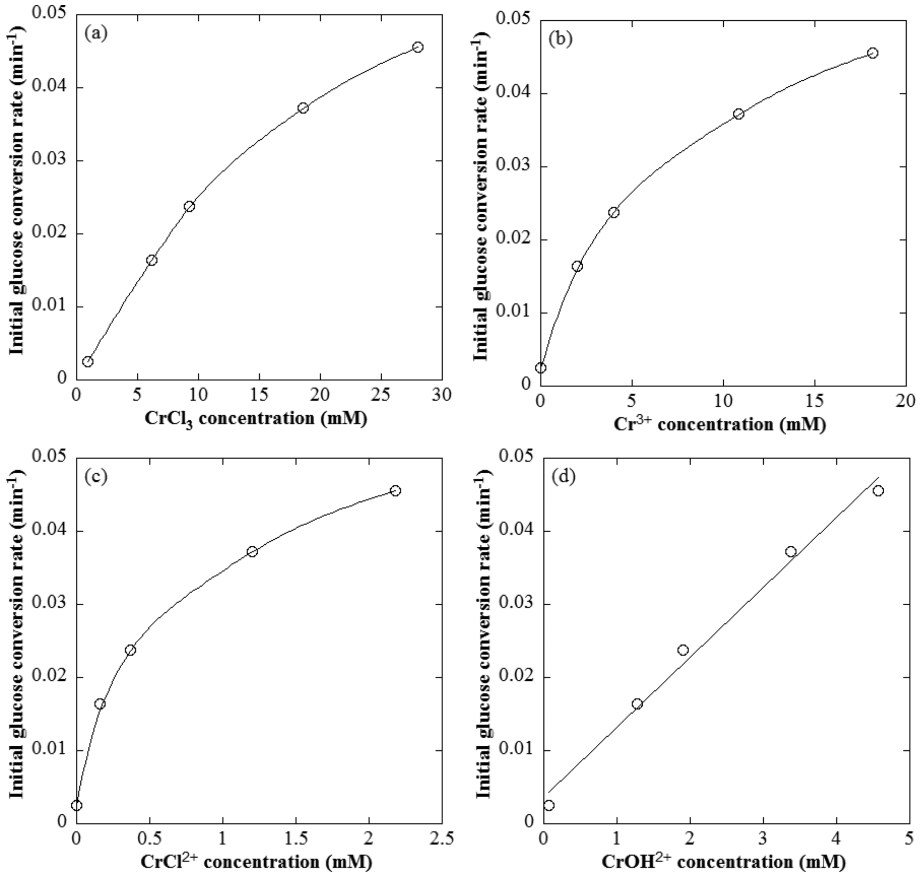


**Figure 7.** Correlation of initial rate of glucose consumption vs the $CrCl_3$ concentration and vs the associated concentrations of various Cr ions predicted from the speciation model using the OLI software. Reaction conditions: initial reactant ~10 wt % and 413 K.

(~24% conversion in 10 min; see Figure 4a) compared to the $CrCl_3$ only case (~32% conversion in 10 min; see Figure 1a). That is, Brønsted acidity inhibits the Lewis acid-catalyzed isomerization of aldoses. This experimental observation combined with the above-discussed trends in the $CrCl_3$ speciation in the presence of HCl suggests that $CrOH^{2+}$ could be the most active species for the isomerization, as it is the only Cr species whose formation is suppressed in the presence of HCl (in the range 0−0.1 M).

To further correlate the rate of glucose consumption with the various Cr species, a series of kinetics experiments starting with glucose and varying $CrCl_3$ concentrations was conducted. The initial rates (at $t = 0$) of glucose consumption were obtained by fitting the glucose concentration profiles at short times with a first-order rate expression. These rates are plotted in Figure 7 as a function of the concentrations of various Cr species calculated using the OLI software at the $CrCl_3$ concentration and temperature of the reaction. It is apparent that the rate of glucose consumption scales linearly with the $CrOH^{2+}$ concentration (Figure 7d), whereas nonlinear trends are found with the concentration of the other Cr species (Figure 7a−c). The linear scaling of glucose consumption rate with the concentration of $CrOH^{2+}$ further corroborates that $CrOH^{2+}$ is the most active Cr species for glucose isomerization.

We also investigated $AlCl_3$-catalyzed glucose transformation to assess whether the observations here can be extended to other salts (Lewis acids) that are active for the glucose isomerization. It was found that $Al^{3+}$ and $Al(OH)^{2+}$ are the dominant species in the $AlCl_3$ speciation and the $Al(OH)^{2+}$ concentration drops upon adding HCl (see Figure S1a), similar to the trends observed in the $CrCl_3$ speciation. Also, the addition of HCl to $AlCl_3$ adversely affects the glucose disappearance rate (see Figure S1b), similar to the $CrCl_3$-catalyzed glucose transformation, as shown in Table 1. Overall, these observations clearly indicate that $Al(OH)^{2+}$ is the most active species for the $AlCl_3$-catalyzed isomerization, analogous to $Cr(OH)^{2+}$ in the case of $CrCl_3$. Further, it is observed that the rate of glucose disappearance is slower in the case of $AlCl_3$ (0.014 $min^{-1}$) compared to $CrCl_3$ (0.036 $min^{-1}$) under similar reaction conditions and a metal-to-glucose molar ratio of 3:100 (see Table 1). Here, it should also be noticed that the predicted concentration of $Al(OH)^{2+}$ is lower than that of $Cr(OH)^{2+}$ under similar operating conditions. This could also explain the use of a higher reaction temperature (443 K) in an earlier reported study of $AlCl_3$ (with HCl)-catalyzed HMF production from glucose.[54]

We expect that the −OH on the metal center can assist in the deprotonation step in the aldose-to-ketose isomerization reaction, similar to the Sn-BEA zeolite case.[72,73] A plausible reaction mechanism of Lewis acid-catalyzed glucose (aldose)-to-fructose (ketose) isomerization is included in the Supporting Information (see Scheme S1). Deprotonation at the O2 position activates the glucose molecule to form a complex between glucose and the Lewis acid site, followed by hydride transfer from the C2 to C1 carbon and back proton transfer to O1 to complete the catalytic cycle. This Lewis acid−Brønsted base bifunctional behavior is reminiscent of the open SnOH site in Sn-$\beta$ zeolite[72,74] and could explain the higher activity of $CrOH^{2+}$ compared with the other Cr species. The speciation calculations also show that the $CrOH^{2+}$ concentration increases


dx.doi.org/10.1021/ja3122763 | J. Am. Chem. Soc. 2013, 135, 3997−4006

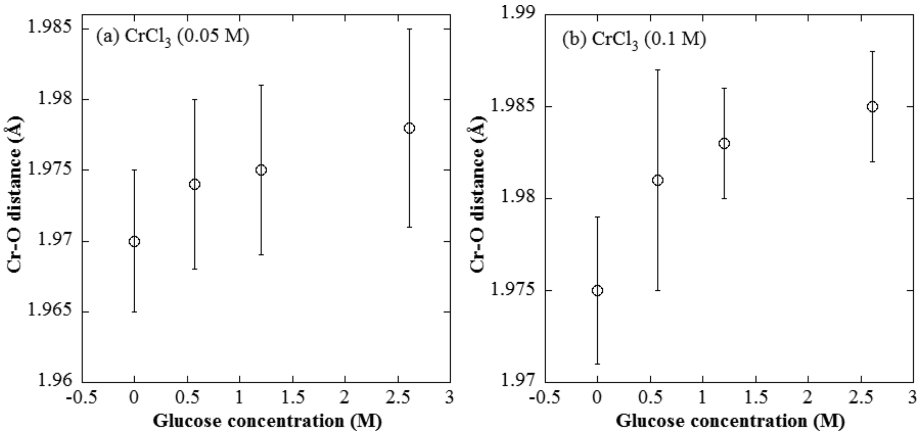


**Figure 8.** EXAFS data showing the effect of glucose addition on the Cr−O distance in water at two different $CrCl_3$ concentrations at room temperature.

with increasing temperature (Supporting Information). This suggests that the reaction temperature plays a dual role in the isomerization reaction: it not only helps in overcoming the activation energy barrier but also generates more catalytically active species that in turn accelerate the isomerization reaction. Also, a recent study showed that tungsten acid dissolves at higher temperature and acts as a homogeneous catalyst in ethylene glycol production from cellulose that precipitates upon cooling.[75] In these regards, speciation models, such as the one employed here, are critical in our ability to quantitatively describe reaction rates and species concentrations in biomass processing.

**Glucose Coordination with the Chromium Ion.** To help elucidate the interaction of the glucose molecule with the metal center, two sets of $CrCl_3$ solutions of concentrations 0.05 and 0.1 M were analyzed using EXAFS spectroscopy, at varying glucose concentrations. When $CrCl_3$ is dissolved in pure water, the Cr(III) cation is surrounded on average by six water molecules, as obtained by the EXAFS analysis. Coordination between the negatively charged oxygen atom of water and the Cr(III) cation is expected at all the times during reaction. For homogeneous catalysis to occur, it is also reasonable to expect that the Cr cation should be in close contact with a glucose molecule, with the glucose molecule replacing water molecules in the first coordination shell. Similar to what occurs in water, oxygen atoms of the glucose hydroxyl groups will coordinate with the metal cation. Since EXAFS cannot distinguish between the oxygen atoms of water and glucose, it is not possible to determine the number of water molecules that have been replaced by glucose. However, since the effective radius (the Stokes radius) of glucose, at 3.6 Å, is larger than that of water (1.35 Å), it is expected that the steric effect from the glucose molecule disturbs the coordination sphere around the chromium ion and increases the average Cr(III) cation−oxygen atom (Cr−O) distance. Such expansion can be, in principle, detected by the EXAFS analysis, and it is evident in our results. Figure 8 shows the effect of glucose addition on the average Cr−O distance obtained from the EXAFS analysis. The Cr−O distance increases with increasing glucose concentration (in the studied range of 0−2.6 M glucose). This could be explained by an increasing number of water molecules being displaced by glucose, indicating the presence of a glucose molecule in the first coordination shell of the Cr cation.

In addition to the EXAFS analysis presented here, the coordination of Cr cation $[Cr(OH)^{2+}]$ with the glucose molecule and water molecules was calculated using CPMD simulations. It has to be noted that the $Cr(OH)^{2+}$−glucose configuration for the CPMD simulations was based on our preliminary calculations with the unhydrolyzed Cr cation. Since two metal centers are required for the enzyme-catalyzed glucose-to-fructose reaction,[76] we initially placed two unhydrolyzed Cr cations coordinated with a glucose molecule (solvated in water). Upon relaxing the system with CPMD simulations at 350 K, we observed that only one Cr remained coordinated to the oxygens (of C1 and C2, as shown in Figure 9a) of the closed-chain glucose molecule. Hence, the configuration with one $Cr(OH)^{2+}$ group placed near the C1 and C2 hydroxyl groups of the glucose molecule, solvated in water, was chosen to investigate the coordination of the hydrolyzed Cr with the glucose molecule and neighboring waters. Details of CPMD simulations are provided in the Supporting Information. The radial pair distribution function and the coordination number between the metal center and the oxygen atoms in the system are shown in Figure 9b. Overall, the metal center is coordinated with six oxygen atoms—consistent with the EXAFS data—in an octahedral structure:

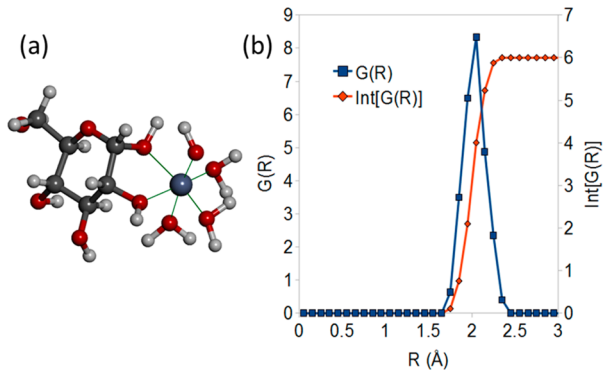


**Figure 9.** (a) Molecular snapshot from the simulation showing the coordination of the $Cr(OH)^{2+}$ cation, the glucose molecule, and water molecules (background waters are not shown for clarity). (b) Radial pair distribution function, $G(R)$, of the $Cr(OH)^{2+}$ cation with oxygen atoms and number integral of $G(R)$. Only the portion of the $G(R)$ showing the first coordination shell is shown here. The number integral of $G(R)$ gives the coordination number of Cr with oxygens. It has to be noted that the radial pair distribution function is calculated on the basis of a short CPMD trajectory of 1 ps.


dx.doi.org/10.1021/ja3122763 | J. Am. Chem. Soc. 2013, 135, 3997−4006

one O from the hydroxyl group, two from the glucose molecule, and the three from water molecules (cf. Figure 9a). The Cr−O distance for the hydroxyl group is significantly shorter than the Cr−O distances of glucose or water since the interaction of the metal cation is much stronger with a negatively charged hydroxyl group than with the oxygen atoms of neutral water or glucose molecules. The average Cr−O(H) distance is 1.89 ± 0.07 Å, whereas the average Cr−O distances for Cr and water oxygens and for Cr and glucose oxygens are 2.06 ± 0.06 and 2.11 ± 0.07 Å, respectively. This is in a qualitative agreement with the EXAFS data reported above. Our simulation results indicate that the presence of glucose displaces water from the active Cr ion as an important step in ring-opening and subsequent isomerization.

## CONCLUSIONS

We have used kinetics experiments, speciation modeling, EXAFS analysis, and CPMD simulation to gain insights into the combined Lewis ($CrCl_3$) and Brønsted (HCl) acid catalysis of aldoses (glucose) to ketoses (fructose) to furans (HMF) to levulinic and formic acids. $CrCl_3$ is found to be an efficient catalyst for glucose isomerization to fructose in aqueous media. The hydrolysis of the Cr(III) ion releases $H^+$ and decreases the solution pH. This Lewis acid-derived (intrinsic) Brønsted acidity is primarily responsible for the fructose dehydration to HMF and its subsequent hydrolysis to levulinic acid at low temperatures when no external Brønsted acids are added. It is also found that the Lewis acid catalyst promotes side reactions and thus increases the overall rate of disappearance of ketoses (fructose) and furans (HMF). As a result, while $CrCl_3$ can isomerize glucose to fructose and drive the Brønsted acid-catalyzed dehydration/rehydration reactions, it is not selective in the HMF and levulinic acid production when used by itself.

For the first time, we propose that, among the various Cr ions generated in aqueous media, $CrOH^{2+}$ is the most active for the aldose-to-ketose isomerization and possibly exhibits a Lewis acid−Brønsted base bifunctional behavior. We also show for the first time that Brønsted acid catalysts inhibit the Lewis acid-catalyzed isomerization by decreasing the concentration of the active Cr species $CrOH^{2+}$ due to a shift in the chemical equilibrium of hydrolysis of the metal cation. A strong interaction between the Cr cation and the glucose molecule in the first coordination sphere of the metal ion is indicated from EXAFS analysis and CPMD simulation, whereby some of the water is displaced in order for ring-opening and isomerization to proceed.

The interplay between the acids indicates that, from a practical standpoint, optimizing the concentrations of Lewis and Brønsted acids in the cascade reactions to maximize the desired products yield is feasible and advisable. For example, high yields of glucose to levulinic acid in a single aqueous phase (46%) and to HMF in a biphasic system (59%) were achieved at a moderate reaction temperature (413 K) by combining $CrCl_3$ (Lewis acid) with HCl (Brønsted acid). Further optimization should be possible by varying additional operating conditions and amounts of catalysts.

## ASSOCIATED CONTENT

### Supporting Information

Comparison between $CrCl_2$- and $CrCl_3$-catalyzed glucose conversion, detailed information about the $CrCl_3$ speciation calculation using the OLI software, complete $CrCl_3$ speciation results, details of the CPMD simulations, results for $AlCl_3$ speciation, as well as reactions and a plausible reaction mechanism for the Lewis acid-catalyzed glucose isomerization. This material is available free of charge via the Internet at http://pubs.acs.org.

## AUTHOR INFORMATION

### Corresponding Author

vlachos@udel.edu; sandler@udel.edu

### Notes

The authors declare no competing financial interest.

## ACKNOWLEDGMENTS

This research is based on work financially supported as part of the Catalysis Center for Energy Innovation, an Energy Frontier Research Center funded by the U.S. Department of Energy, Office of Science, Office of Basic Energy Sciences under award no. DE-SC0001004.

## REFERENCES

(1) Schmidt, L. D.; Dauenhauer, P. J. *Nature* **2007**, *447*, 914.
(2) Alonso, D. M.; Bond, J. Q.; Dumesic, J. A. *Green Chem.* **2010**, *12*, 1493.
(3) Climent, M. J.; Corma, A.; Iborra, S. *Green Chem.* **2011**, *13*, 520.
(4) Vlachos, D. G.; Caratzoulas, S. *Chem. Eng. Sci.* **2010**, *65*, 18.
(5) Stocker, M. *Angew. Chem., Int. Ed.* **2008**, *47*, 9200.
(6) Lewkowski, J. *Arkivoc* **2001**, 2.
(7) James, O. O.; Maity, S.; Usman, L. A.; Ajanaku, K. O.; Ajani, O. O.; Siyanbola, T. O.; Sahu, S.; Chaubey, R. *Energy Environ. Sci.* **2010**, *3*, 1833.
(8) Kuster, B. F. M. *Starch-Starke* **1990**, *42*, 314.
(9) Zakrzewska, M. E.; Bogel-Lukasik, E.; Bogel-Lukasik, R. *Chem. Rev.* **2011**, *111*, 397.
(10) Rackemann, D. W.; Doherty, W. O. S. *Biofuels, Bioprod. Biorefin.* **2011**, *5*, 198.
(11) Peng, L.; Lin, L.; Li, H. *Prog. Chem.* **2012**, *24*, 801.
(12) Serrano-Ruiz, J. C.; West, R. M.; Durnesic, J. A. In *Annual Review of Chemical and Biomolecular Engineering*; Annual Reviews: Palo Alto, CA, Prausnitz, J. M., Doherty, M. F., Segalman, M. A., Eds.; **2010**; Vol. *1*, p 79.
(13) Vandam, H. E.; Kieboom, A. P. G.; Vanbekkum, H. *Starch-Starke* **1986**, *38*, 95.
(14) Roman-Leshkov, Y.; Chheda, J. N.; Dumesic, J. A. *Science* **2006**, *312*, 1933.
(15) Rigal, L.; Gaset, A.; Gorrichon, J. P. *Ind. Eng. Chem. Prod. Res. Dev.* **1981**, *20*, 719.
(16) Chuntanapum, A.; Yong, T. L. K.; Miyake, S.; Matsumura, Y. *Ind. Eng. Chem. Res.* **2008**, *47*, 2956.
(17) Bicker, M.; Hirth, J.; Vogel, H. *Green Chem.* **2003**, *5*, 280.
(18) Brown, D. W.; Floyd, A. J.; Kinsman, R. G.; Roshanali, Y. *J. Chem. Technol. Biotechnol.* **1982**, *32*, 920.
(19) Moreau, C.; Durand, R.; Razigade, S.; Duhamet, J.; Faugeras, P.; Rivalier, P.; Ros, P.; Avignon, G. *Appl. Catal., A* **1996**, *145*, 211.
(20) Kruger, J. S.; Nikolakis, V.; Vlachos, D. G. *Curr. Opin. Chem. Eng.* **2012**, *1*, 312.
(21) Choudhary, V.; Burnett, R. I.; Vlachos, D. G.; Sandler, S. I. *J. Phys. Chem. C* **2012**, *116*, 5116.
(22) Zhao, H.; Holladay, J. E.; Brown, H.; Zhang, Z. C. *Science* **2007**, *316*, 1597.
(23) Mascal, M.; Nikitin, E. B. *Chemsuschem* **2009**, *2*, 423.
(24) Lew, C. M.; Rajabbeigi, N.; Tsapatsis, M. *Ind. Eng. Chem. Res.* **2012**, *51*, 5364.
(25) Boisen, A.; Christensen, T. B.; Fu, W.; Gorbanev, Y. Y.; Hansen, T. S.; Jensen, J. S.; Klitgaard, S. K.; Pedersen, S.; Riisager, A.; Stahlberg, T.; Woodley, J. M. *Chem. Eng. Res. Des.* **2009**, *87*, 1318.
(26) Chheda, J. N.; Roman-Leshkov, Y.; Dumesic, J. A. *Green Chem.* **2007**, *9*, 342.
(27) Asghari, F. S.; Yoshida, H. *Ind. Eng. Chem. Res.* **2006**, *45*, 2163.

(28) Bicker, M.; Kaiser, D.; Ott, L.; Vogel, H. *J. Supercrit. Fluids* **2005**, *36*, 118.
(29) Shimizu, K.; Uozumi, R.; Satsuma, A. *Catal. Commun.* **2009**, *10*, 1849.
(30) Qi, X. H.; Watanabe, M.; Aida, T. M.; Smith, R. L. *Ind. Eng. Chem. Res.* **2008**, *47*, 9234.
(31) Qi, X. H.; Watanabe, M.; Aida, T. M.; Smith, R. L. *Catal. Commun.* **2009**, *10*, 1771.
(32) Wang, F. F.; Shi, A. W.; Qin, X. X.; Liu, C. L.; Dong, W. S. *Carbohydr. Res.* **2011**, *346*, 982.
(33) Zhang, Z. H.; Liu, B.; Zhao, Z. B. *Carbohydr. Polym.* **2012**, *88*, 891.
(34) Shi, C.; Zhao, Y.; Xin, J.; Wang, J.; Lu, X.; Zhang, X.; Zhang, S. *Chem. Commun.* **2012**, *48*, 4103.
(35) Jadhav, A. H.; Kim, H.; Hwang, I. T. *Catal. Commun.* **2012**, *21*, 96.
(36) Torres, A. I.; Tsapatsis, M.; Daoutidis, P. *Comput. Chem. Eng.* **2012**, *42*, 130.
(37) Hu, S.; Zhang, Z.; Song, J.; Zhou, Y.; Han, B. *Green Chem.* **2009**, *11*, 1746.
(38) Yong, G.; Zhang, Y. G.; Ying, J. Y. *Angew. Chem., Int. Ed.* **2008**, *47*, 9345.
(39) Sievers, C.; Musin, I.; Marzialetti, T.; Olarte, M. B. V.; Agrawal, P. K.; Jones, C. W. *Chemsuschem* **2009**, *2*, 665.
(40) Binder, J. B.; Raines, R. T. *J. Am. Chem. Soc.* **2009**, *131*, 1979.
(41) Ohara, M.; Takagaki, A.; Nishimura, S.; Ebitani, K. *Appl. Catal., A* **2010**, *383*, 149.
(42) Rasrendra, C.; Soetedjo, J.; Makertihartha, I.; Adisasmito, S.; Heeres, H. *Top. Catal.* **2012**, *55*, 543.
(43) Dutta, S.; De, S.; Alam, M. I.; Abu-Omar, M. M.; Saha, B. *J. Catal.* **2012**, *288*, 8.
(44) Moliner, M.; Roman-Leshkov, Y.; Davis, M. E. *Proc. Natl. Acad. Sci. U.S.A.* **2010**, *107*, 6164.
(45) Roman-Leshkov, Y.; Moliner, M.; Labinger, J. A.; Davis, M. E. *Angew. Chem., Int. Ed.* **2010**, *49*, 8954.
(46) Choudhary, V.; Pinar, A. B.; Sandler, S. I.; Vlachos, D. G.; Lobo, R. F. *ACS Catal.* **2011**, *1*, 1724.
(47) Nikolla, E. N. E.; Roman-Leshkov, Y.; Moliner, M.; Davis, M. E. *ACS Catal.* **2011**, *1*, 408.
(48) Rasrendra, C. B.; Makertihartha, I. G. B. N.; Adisasmito, S.; Heeres, H. J. *Top. Catal.* **2010**, *53*, 1241.
(49) Efremov, A.; Pervyshina, G.; Kuznetsov, B. *Chem. Nat. Compd.* **1998**, *34*, 182.
(50) Peng, L.; Lin, L.; Zhang, J.; Zhuang, J.; Zhang, B.; Gong, Y. *Molecules* **2010**, *15*, 5258.
(51) Tyrlik, S. K.; Szerszen, D.; Kurzak, B.; Bal, K. *Starch-Starke* **1995**, *47*, 171.
(52) Tyrlik, S. K.; Szerszen, D.; Olejnik, M.; Danikiewicz, W. *J. Mol. Catal. A: Chem.* **1996**, *106*, 223.
(53) De, S.; Dutta, S.; Saha, B. *Green Chem.* **2011**, *13*, 2859.
(54) Pagan-Torres, Y. J.; Wang, T.; Gallo, J. M. R.; Shanks, B. H.; Dumesic, J. A. *ACS Catal.* **2012**, *2*, 930.
(55) Newville, M. *J. Synchrotron Radiat.* **2001**, *8*, 322.
(56) Ravel, B.; Newville, M. *J. Synchrotron Radiat.* **2005**, *12*, 537.
(57) Zabinsky, S. I.; Rehr, J. J.; Ankudinov, A.; Albers, R. C.; Eller, M. J. *Phys. Rev. B* **1995**, *52*, 2995.
(58) Wang, P. M.; Anderko, A.; Young, R. D. *Fluid Phase Equilib.* **2002**, *203*, 141.
(59) Wang, P.; Springer, R. D.; Anderko, A.; Young, R. D. *Fluid Phase Equilib.* **2004**, *222*, 11.
(60) Wang, P.; Anderko, A.; Springer, R. D.; Young, R. D. *J. Mol. Liq.* **2006**, *125*, 37.
(61) Kosinski, J. J.; Wang, P.; Springer, R. D.; Anderko, A. *Fluid Phase Equilib.* **2007**, *256*, 34.
(62) Laio, A.; Gervasio, F. L. *Rep. Prog. Phys.* **2008**, 71.
(63) Patil, S. K. R.; Heltzel, J.; Lund, C. R. F. *Energy Fuels* **2012**, *26*, 5281.
(64) Horvat, J.; Klaic, B.; Metelko, B.; Sunjic, V. *Croat. Chem. Acta* **1986**, *59*, 429.
(65) Choudhary, V.; Sandler, S. I.; Vlachos, D. G. *ACS Catal.* **2012**, *2*, 2022.
(66) Weingarten, R.; Tompsett, G. A.; Conner, W. C., Jr.; Huber, G. W. *J. Catal.* **2011**, *279*, 174.
(67) Nikbin, N.; Caratzoulas, S.; Vlachos, D. G. *Chemcatchem* **2012**, *4*, 504.
(68) Asghari, F. S.; Yoshida, H. *Ind. Eng. Chem. Res.* **2007**, *46*, 7703.
(69) Roman-Leshkov, Y.; Dumesic, J. A. *Top. Catal.* **2009**, *52*, 297.
(70) Bailar, J. C., Emeléus, H. J., Nyholm, R, Trotman-Dickenson, A. F., Eds. *Comprehensive Inorganic Chemistry*; Pergamon Press: Oxford, 1973; Vol. 3.
(71) Pechova, A.; Pavlata, L. *Vet. Med. (Prague, Czech Repub.)* **2007**, *52*, 1.
(72) Bermejo-Deval, R.; Assary, R. S.; Nikolla, E.; Moliner, M.; Roman-Leshkov, Y.; Hwang, S.-J.; Palsdottir, A.; Silverman, D.; Lobo, R. F.; Curtiss, L. A.; Davis, M. E. *Proc. Natl. Acad. Sci. U.S.A.* **2012**, *109*, 9727.
(73) Choudhary, V.; Caratzoulas, S.; Vlachos, D. G. *Carbohydr. Res.* **2013**, *368*, 89.
(74) Boronat, M.; Concepcion, P.; Corma, A.; Renz, M.; Valencia, S. *J. Catal.* **2005**, *234*, 111.
(75) Tai, Z.; Zhang, J.; Wang, A.; Zheng, M.; Zhang, T. *Chem. Commun.* **2012**, *48*, 7052.
(76) Bennett, B. C.; Yeager, M. *Structure* **2010**, *18*, 657.